PHYSICAL REVIEW B **75**, 081405(R) (2007)

Scattering coefficients of surface plasmon polaritons impinging at oblique incidence onto one-dimensional surface relief defects

A. Yu. Nikitin[1,2,*] and L. Martín-Moreno[1,†]

[1]*Departamento de Física de la Materia Condensada-ICMA, Universidad de Zaragoza, E-50009 Zaragoza, Spain*

[2]*Theoretical Physics Department, A.Ya. Usikov Institute for Radiophysics and Electronics, Ukrainian Academy of Sciences, 12 Acad. Proskura Str., 61085 Kharkov, Ukraine*

(Received 19 December 2006; revised manuscript received 6 February 2007; published 28 February 2007)

We present a theoretical analysis of surface plasmon polariton (SPP) scattering by shallow one-dimensional surface relief defects for oblique incidence, applying both surface impedance boundary conditions and Rayleigh expansion. Using this method, nontrivial angular dependences for transmission, reflection, and out-of-plane scattering are obtained. For the case of a defect with rectangular shape, we give an analytical description of the interference phenomena caused by the SPP diffraction for both a single defect (either protrusion or indentation) and a finite array of them.

DOI: 10.1103/PhysRevB.75.081405 PACS number(s): 73.20.Mf, 78.67.−n, 41.20.Jb

Diffraction methods, developed so far for the scattering of electromagnetic waves, are now being transferred to the case of surface electromagnetic waves [surface plasmon polaritons (SPPs), existing at the metal boundaries]. These waves are striking due to their high localization near the interface (up to subwavelength scales) and high field intensities, which may lead to many applications. Propagation of SPPs can be modified by patterning the surface in which they propagate. In recent years plasmonic elements such as mirrors, subwavelength waveguides, and emitters have been studied experimentally.[1–5] Still, even for the case of scatterers with translational symmetry in one direction (grooves or ridges), the theory is incomplete, most works being devoted to the case of normal incidence.[6–8] To our knowledge, the scattering at non-normal incidence has been addressed theoretically for the cases of thin films,[4] the boundary to a uniform medium,[9] and chains of nanoparticles,[10] but not for SPPs in optically thick films. Notably, most experiments consider oblique incidence, as the extraction of reflection coefficients is easier in this case. The aim of this Rapid Communication is to partially close this gap, addressing theoretically the angular dependence of SPP scattering by shallow relief corrugations.

Consider a surface plasmon of unit amplitude with frequency ω (wavelength λ), propagating with wave vector $\mathbf{k}_p$ along a lossless metal,[11] and impinging at angle θ onto a one-dimensional (1D) relief perturbation, $z=h(x)$, uniform in the y direction; see Fig. 1. The dielectric permittivity of the metal, bounding with the vacuum, is ϵ (the surface impedance is $\xi=1/\sqrt{\epsilon}$). In this Rapid Communication, we consider shallow reliefs $|h|\ll\lambda$. For this case the Rayleigh expansion, which expresses the scattered field in all spatial regions in terms of *only* upward moving plane waves, is a good approximation.[12] Within this expansion the total electric field in the vacuum half-space has the form

$$\mathbf{E}(\mathbf{r}) = \mathbf{e}_p \exp(i\mathbf{k}_p \cdot \mathbf{r}) + \int d k \mathbf{E}_k \exp(i\mathbf{K} \cdot \mathbf{r}), \qquad (1)$$

where $\mathbf{k}_p = g(q_p \cos\theta, q_p \sin\theta, \xi)$, $q_p = \sqrt{1-\xi^2}$, $g=\omega/c = 2\pi/\lambda$, and the wave vectors of scattered plane waves are $\mathbf{K}=(k, gq_p \sin\theta, k_z)$ with z components $k_z = \sqrt{g^2-(gq_p \sin\theta)^2-k^2}$ satisfying the radiation condition $\mathrm{Im}(k_z)\geqslant 0$. The unit vector along the electric field of the incoming SPPs is $\mathbf{e}_p=(\xi\cos\theta, \xi\sin\theta, -q_p)$. Within the surface impedance boundary conditions (SIBC),[13] valid for $|\xi| \ll 1$, the magnetic, $\mathbf{H}(\mathbf{r})$, and the electric fields at the surface must satisfy

$$\mathbf{E}_t(\mathbf{r}) + \xi[\mathbf{n}(x) \times \mathbf{H}(\mathbf{r})] = 0 \text{ at } z = h(x), \qquad (2)$$

where $\mathbf{E}_t = \mathbf{E} - \mathbf{n}(\mathbf{n}\cdot\mathbf{E})$ is the tangential component of the electric field and $\mathbf{n}$ is the surface normal unitary vector (pointing towards the metal). Substituting the expressions for $\mathbf{E}$ and $\mathbf{H}$ into Eq. (2) results in a pair of coupled integral equations describing the SPP-defect interaction:

$$r_q^\sigma + \sum_{\sigma'} \int dq' U_{qq'}^{\sigma\sigma'} G_{q'}^{\sigma'} r_{q'}^{\sigma'} = -U_{qq_{px}}^{\sigma-}, \qquad (3)$$

where $q=k/g$, $q_{px}=q_p\cos\theta$, and the binary variable $\sigma=+$ $(-)$ corresponds to s (p) polarizations. The renormalized field amplitudes r_q^σ, are related to $\mathbf{E}_k$ through the Fourier transformations of the Green's functions corresponding to p polarization, $G_q^- = 1/(\xi+q_z)$ (where $q_z=k_z/g$), and s polarization, $G_q^+ = 1/(1+\xi q_z)$, as follows:

$$\mathbf{E}_k = g^{-1} \sum_\sigma G_q^\sigma r_q^\sigma \mathbf{e}_q^\sigma. \qquad (4)$$

Here the polarization unit vectors for each plane wave are $\mathbf{e}_q^+ = \mathbf{e}_z \times \mathbf{q}_t/q_t$ and $\mathbf{e}_q^- = \mathbf{e}_q^+ \times \mathbf{K}/g$ with $\mathbf{q}_t=(q, q_p\sin\theta, 0)$. The potential in these equations, $U_{qq'}^{\sigma\sigma'}$, may be greatly simplified if, analogously to Ref. 14, we expand the boundary condition over the parameters $|\partial_x h|$ and h/λ. Remarkably, retaining only first-order terms in the expansion already provides an excellent fulfillment of energy conservation even in the cases where the surface corrugations possess abrupt edges. Keeping only these terms, we arrive at the following simplified potential:

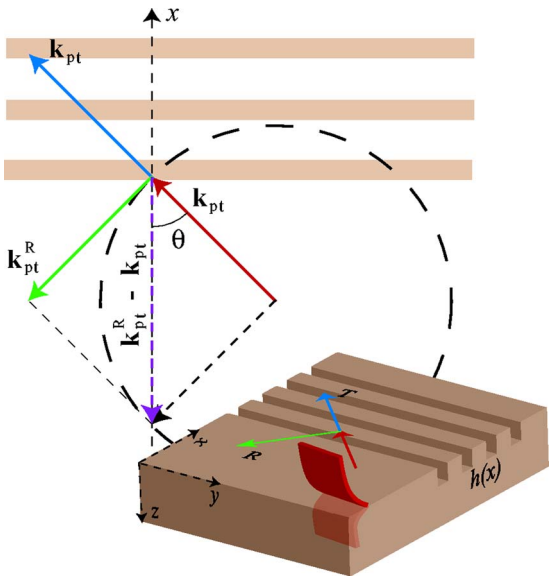

FIG. 1. (Color online) Schematic illustration of the studied system: SPP scattering at the inhomogeneity formed by the perturbation of the interface profile $h(x)$. By the solid arrows the wave vectors of the incoming, reflected, and transmitted SPPs are shown.

$$U^{\sigma\sigma'}_{qq'} = -\sigma'^{(1+\sigma)/2}\eta_{q-q'}\left(\frac{S^{\sigma\cdot\sigma'}_{qq'}}{G^{-\sigma'}_{q'}} - \delta_{\sigma,\sigma'}\xi^{(1+\sigma')/2}q_t q'_t\right), \quad (5)$$

where $\delta_{\sigma,\sigma'}$ is the Kronecker symbol and $S^{+}_{qq'}=\mathbf{q}_t\cdot\mathbf{q}'_t/q_t q'_t$ and $S^{-}_{qq'}=\mathbf{e}_z\cdot(\mathbf{q}_t\times\mathbf{q}'_t)/q_t q'_t$ are the cosine and sine of the angle formed by the vectors $\mathbf{q}_t$ and $\mathbf{q}'_t$, respectively. $\eta_q = ig^2 h_q$, with h_q being the Fourier image of $h(x)$. Solving Eq. (3) and using the relation (4), we can find the electromagnetic field at any point of the vacuum half-space. However, for the SPP reflection and transmission coefficients only the fields in the far zone are necessary. These asymptotic fields may be obtained by integrating Eq. (1) in the complex plane:

$$\mathbf{E}(\mathbf{r}) = \mathbf{e}_p(1+\tau)\exp(i\mathbf{k}_p\cdot\mathbf{r}), \quad x\to\infty,$$

$$\mathbf{E}(\mathbf{r}) = \mathbf{e}_p\exp(i\mathbf{k}_p\cdot\mathbf{r}) + \rho\mathbf{e}^{-}_{-q_{px}}\exp(i\mathbf{k}^R_p\cdot\mathbf{r}), \quad x\to-\infty.$$

Here $\mathbf{k}^R_p = g(-q_{px}, q_p\sin\theta, \xi)$ is the wave vector of the reflected SPP; the amplitudes of the reflected and transmitted SPPs are

$$\rho = \frac{2\pi i\xi}{q_{px}}r^{-}_{-q_{px}}, \quad 1+\tau = 1+\frac{2\pi i\xi}{q_{px}}r^{-}_{q_{px}}. \quad (6)$$

The reflection, $R=|\rho|^2$, and transmission, $T=|1+\tau|^2$, coefficients together with the out-of-plane scattering coefficient S,

$$S = \frac{4\pi|\xi|}{q_{px}}\sum_{\sigma}\int_{\mathrm{Im}(q_z)=0} dqq_z|G^{\sigma}_{q}r^{\sigma}_{q}|^2, \quad (7)$$

satisfy the energy conservation law $1-R-T-S=0$. Note that, at oblique incidence, both p-polarized and s-polarized homogeneous waves contribute to the out-of-plane scattering. The

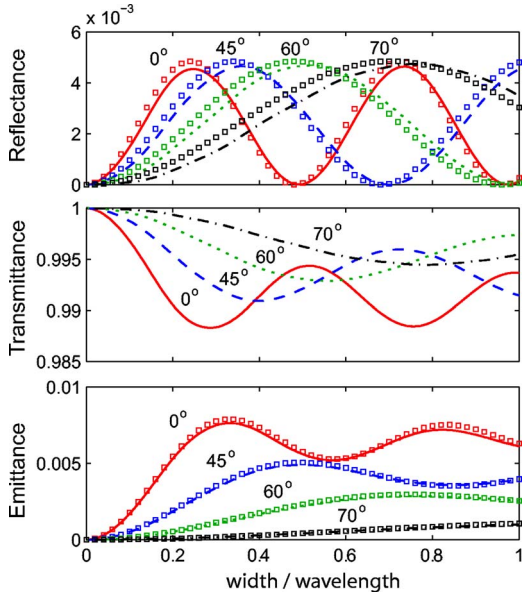

FIG. 2. (Color online) The dependences of the reflectance R, the transmittance T, and the out-of-plane emittance S upon the parameter a/λ at different incident angles θ for SPP scattering by a single rectangular indentation of the depth $w/\lambda=0.02$. $\xi=-0.277i$ (Ag at 600 nm).

vector angular dependence of the power radiated out of plane is given by the differential reflection coefficient (DRC), which is the integrand in Eq. (7) (after the change of variable q to the polar angle in the x-y plane).

The solution of the coupled integral equations may be obtained both numerically and analytically (as a Born expansion in the amplitude of the defect, whenever this expansion converges). In the latter case the nth-order term is proportional to the nth power of the defect Fourier image, $r^{\sigma(n)}_{q} \sim \eta^n$. As the analysis shows, the solution within the first-order Born approximation (FOBA) already gives good energy conservation.[15] The solution of Eq. (3) in the FOBA is

$$r^{\sigma(1)}_{q} = -U^{\sigma-}_{qq_{px}} = -\sigma q_p\eta_{q-q_{px}}(q_p S^{-\sigma}_{qq_{px}} - q_t\delta_{\sigma,-}).$$

Taking into account that for the defect of a rectangular shape with amplitude w and width a the Fourier transformation is $\eta_q = igw\sin(qga/2)/\pi q$, we can write the *reflection coefficient for a single defect* R_S in the FOBA as

$$R_S = 4|r|^2\sin^2\left(2\pi q_p\frac{a}{\lambda}\cos\theta\right), \quad r = 2\pi\xi\frac{w}{\lambda}. \quad (8)$$

Here r is the reflection coefficient, which we associate with the SPP reflection from a Heaviside step function. Indeed, the renormalized Fourier image of the surface relief step with the amplitude w is $\eta_q = gw/2\pi q$, which leads to $R=|r|^2$. Similarly, expressions for the DRC, S, and T can be straightforwardly found. The calculations of R, T, and S in the FOBA (square symbols) for the case of a single 1D scatterer of rectangular shape are rendered in Fig. 2, together with the results obtained from solving numerically Eq. (3). We have chosen a fixed wavelength in order to clearly show the geometrical dependences. While the reflectance is not a monoto-

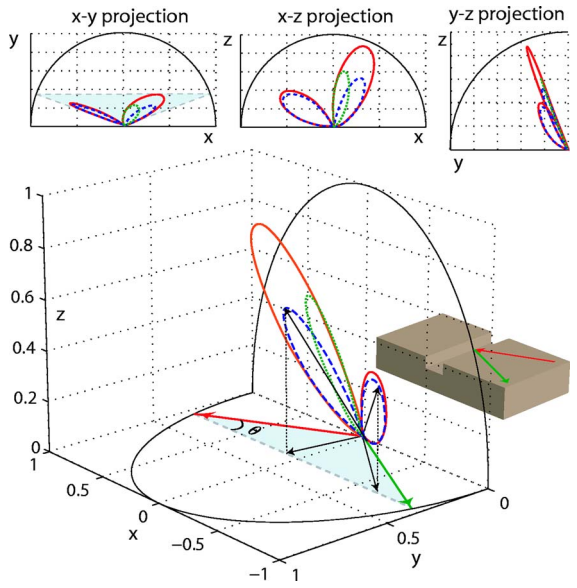

FIG. 3. (Color online) DRC for the rectangular indentation with the width $a/\lambda=0.8$ and the depth $w/\lambda=0.02$, corresponding to SPP scattering at $\theta=20°$. $\xi=-0.277i$ (Ag at 600 nm). The blue shaded angular segment corresponds to the possible tangential components of the homogeneous waves. The dotted (dashed) line is for s (p) polarized waves; the solid curve is the total DRC (all plotted values are normalized to the maximal value of the total DRC).

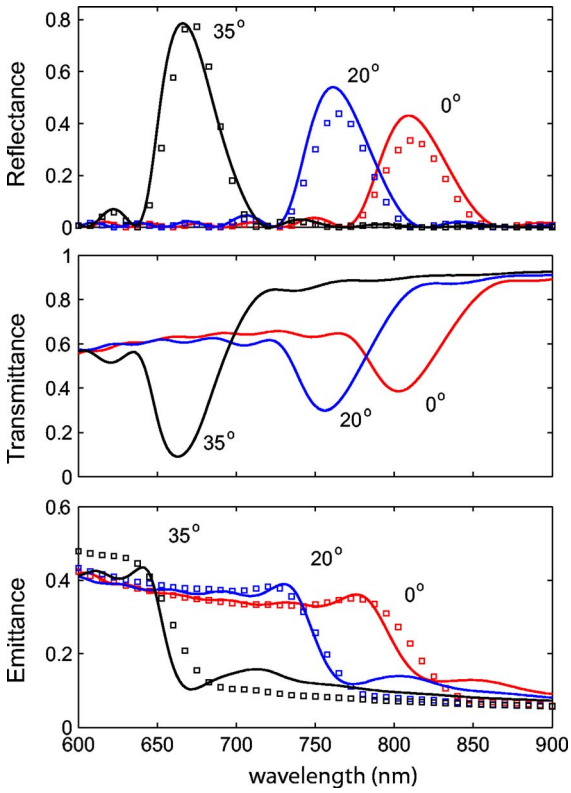

FIG. 4. (Color online) Dependences on the SPP angle of incidence for the reflection (R), transmission (T), and out-of-plane scattering (S) spectra, for an ordered array of $N=8$ scatterers in silver. The period of the array is $d=800$ nm and the scatterers' width $a=200$ nm. The indentation depth is $w=40$ nm. The reflection in the FOBA (which is shown by the square symbols) in Eq. (10) is normalized by an appropriate coefficient so that it coincides with the full numerical calculations in the maxima at $\theta=35°$.

nous function of the angle of incidence, the emittance decreases with increasing θ, so in-plane scattering dominates for large angles of incidence. Notice that, within the FOBA, indentations and protrusions of the same shape have the same scattering coefficients. We have found that, whenever the Rayleigh expansion is valid (i.e., whenever it provides energy conservation) these scattering coefficients are very similar even when the Born series breaks down.

In order to get further insight into SPP scattering and to further justify the interpretation of r, we compare expression (8) with the one obtained for the reflection of a plane electromagnetic (EM) wave (propagating in a 3D media with dielectric constant $\epsilon_1=1$) by a dielectric slab. If the slab has width a and the dielectric constant $\epsilon_2=1+\varepsilon$, which is slightly different from vacuum, the reflectance R^{σ}_{slab} in the case when $|\varepsilon| \ll |\cos\theta|$ is

$$R^{\sigma}_{slab} \simeq 4|r^{\sigma}_f|^2 \sin^2(2\pi\beta a/\lambda), \quad r^{\sigma}_f \simeq -\sigma\frac{\varepsilon(\cos 2\theta)^{(1-\sigma)/2}}{4\cos^2\theta},$$

where $\sigma=+$ $(-)$ is for s (p) polarization, $\beta=\sqrt{\epsilon_2-\sin^2\theta} \simeq \cos\theta$ is the dimensionless x component of the wave vector (the axis Ox is perpendicular to the layer surface), and r^{σ}_f is the amplitude Fresnel reflection coefficient from a single boundary between the dielectrics. Comparing Eqs. (8) and (9) allows the identification of the sine function as arising from the waves reflected at the defect boundaries. Notice that the analogy between the 3D case (s or p polarization) and the 2D SPP case stops here: different EM field components are dominant in these different systems, resulting in different angular dependences for the scattering coefficients. Notably, our result for the SPP reflection off a single relief boundary is that it does not depend on the angle of incidence. This is in keeping with the fact that, in SPPs, the z component of the electric field dominates and this component does not change with in-plane angle of incidence.

For oblique SPP incidence, both s- and p-polarized propagating waves are scattered out of the x-z plane; the precise distribution depends on both the defect geometrical parameters and angle of incidence. Figure 3 renders the polarization and angular distribution of radiated power for a typical case, showing that the directions at which maximum radiation occurs are different for s and p polarization.

Having studied the single-defect case, we consider now the case of a finite periodic array of N protrusions or indentations [each one of them is characterized by a relief $z=h(x)$] located along the Ox axis. Let d be the distance between neighboring defects. Then the Fourier image of this array of scatterers is

$$h^{(N)}_k = h_k \varphi_N(k), \quad \varphi_N(k) = \sum_{n=1}^{N} \exp[ik(n-1)d]. \qquad (9)$$

Within the FOBA, we find that the reflectance for an array of defects can be related to the single-defect reflectance R_S as

$$R = R_S|\varphi_N(-gq_p \cos\theta)|^2. \quad (10)$$

Figure 4 renders the scattering coefficients for SPP scattering by the array of eight defects with rectangular shape. The distance between the defects is $d=800$ nm, and the depth and width of the indentations are $w=40$ nm and $a=200$ nm, correspondingly, which are typical experimental values. The considered metal is silver, where the real part of the dielectric constant is taken from Ref. 16.

Analogously to the case of a normal incidence,[8] maximum reflectance in the array occurs at the low-λ edge of the SPP transmission gap, which is given by the folding of the dispersion relation in a *flat* surface: $\lambda_{max}=2dq_p \cos\theta/m$, where m is an integer. The approximation given by Eq. (10) can also be used to obtain the gap width. After some algebraic manipulations, we obtain that $\Delta\lambda$ decreases as the angle of incidence increases, scaling as $\Delta\lambda \sim \cos\theta$. This is in agreement with the numerical results presented in Fig. 4. With respect to the reflectance maxima, the FOBA predicts an N^2 dependence which breaks down for moderate N ($N \simeq 10$ which is a typical experimental value), higher-order terms being then important, leading to a saturation in the maximum reflectance obtainable.[3,8] Due to this overestimation, for large N the FOBA does not show good quantitative agreement with the full calculation. However, if this is corrected by an N-dependent multiplicative factor [in Eq. (10)], the FOBA captures well both the wavelength and the angular dependence of the reflectance (see Fig. 4). Notice also that when the angle of incidence increases, the reflectivity peak value $R_{max} \sim |\xi|^2/\cos^2\theta$ increases due to two reasons. First R is inversely proportional to $\cos^2\theta$, reflecting the dependence of the scattering cross section in $(w/\lambda)^2$ and the Bragg condition for the resonant wavelength. Second, it is quadratic with respect to the surface impedance modulus (reflecting the degree of confinement of the SPPs on the metal surface), which increases when the resonant wavelength decreases. All the discussed dependencies are the same in the vicinity of any transmission gaps, irrespectively of the band index they originate from.

Notice that the Rayleigh approximation prediction that shallow protrusions and indentations of the same shape have similar scattering coefficients is in apparent contradiction to the results reported in Ref. 3. However, those experiments were performed for *thin films*, where the presence of indentations increases the radiation channel across the metal. In fact, we find good quantitative agreement with the results in Ref. 3 for the case of protrusions, when the leakage radiation through the metal film is small.

To summarize, we have considered the scattering properties of SPPs by defects with translational symmetry in one direction in the case of oblique incidence, providing analytical results for the angular dependence of the scattering coefficients. For single scatterers, we have shown that the reflectance is not a monotonous function of the angle of incidence, while the out-of-plane emittance decreases with it. In the case of multiple scatterers, reflectance maxima increase when the incident angle increases, reflecting the decrease in resonant wavelength (corresponding to Bragg's condition), which both increases the w/λ ratio and decreases the absolute value of ϵ. High reflectance can be obtained for small scatterers and moderate N, which is in agreement with experiments.

The authors acknowledge financial support from the INTAS YS Grant No. 05-109-5206, the European Network of Excellence Plasmo-Nano-Devices (Grant No. FP6-2002-IST-1-507879), the STREP "Surface Plasmon Photonics" (Grant No. FP6-NMP4-CT2003-505699), and the Spanish MCyT Project No. MAT2005-06608-C02.

*Electronic address: alexeynik@rambler.ru

†Electronic address: lmm@unizar.es

[1] J.-C. Weeber, J. R. Krenn, A. Dereux, B. Lamprecht, Y. Lacroute, and J. P. Goudonnet, Phys. Rev. B **64**, 045411 (2001).

[2] W. L. Barnes, A. Dereux, and T. W. Ebbesen, Nature (London) **424**, 824 (2003).

[3] M. U. González, J.-C. Weeber, A.-L. Baudrion, A. Dereux, A. L. Stepanov, J. R. Krenn, E. Devaux, and T. W. Ebbesen, Phys. Rev. B **73**, 155416 (2006).

[4] A. Drezet, A. L. Stepanov, A. Hohenau, B. Steinberger, N. Galler, H. Ditlbacher, A. Leitner, F. R. Aussenegg, J. R. Krenn, M. U. Gonzalez, and J.-C. Weeber, Europhys. Lett. **74**, 693 (2006).

[5] J. Gómez Rivas, M. Kuttge, H. Kurz, P. Haring Bolivar, and J. A. Sánchez-Gil, Appl. Phys. Lett. **88**, 082106 (2006).

[6] J. A. Sánchez-Gil, Appl. Phys. Lett. **73**, 3509 (1998).

[7] J. A. Sánchez-Gil and A. A. Maradudin, Phys. Rev. B **60**, 8359 (1999).

[8] F. López-Tejeira, F. J. García-Vidal, and L. Martín-Moreno, Phys. Rev. B **72**, 161405(R) (2005).

[9] R. Gordon, Phys. Rev. B **74**, 153417 (2006).

[10] A. B. Evlyukhin, S. I. Bozhevolnyi, A. L. Stepanov, and J. R. Krenn, Appl. Phys. B: Lasers Opt. **84**, 29 (2006).

[11] While absorption is not expected to be important for system sizes smaller than the propagation length, neglecting it greatly simplifies the description, as scattering channels are then well defined at large distances.

[12] L. Tsang, J. A. Kong, and K.-H. Ding, *Scattering of Electromagnetic Waves* (Wiley, New York, 2000).

[13] L. D. Landau, E. M. Lifshitz, and L. P. Pitaievskii, *Electrodynamics of Continuous Media*, 2nd ed. (Pergamon Press, New York, 1984).

[14] A. Yu. Nikitin, F. López-Tejeira, and L. Martín-Moreno, Phys. Rev. B **75**, 035129 (2007).

[15] For $|\eta| \gtrsim 1$ the Born approximation breaks down and a numeric solution of Eq. (3) is necessary. Notice that, as $|\eta| \sim ga$ (where a, is the defect width), if the defect is wide enough, $|\eta|$, becomes large even for shallow and smooth reliefs.

[16] *Handbook of Optical Constants of Solids*, edited by E. D. Palik (Academic Press, New York, 1985).